

# Explicit Model Predictive Control of PMSM Drives

Květoslav Belda

*Adaptive Systems dept., The Czech Academy of Sciences  
Institute of Information Theory and Automation*

Pod Vodárenskou věží 4, 182 00 Prague 8, Czech Republic  
belda@utia.cas.cz, <https://orcid.org/0000-0002-1299-7704>

Pavel Píša

*Control Engineering dept., Faculty of Electrical Engineering  
The Czech Technical University in Prague*

Karlovo náměstí 13, 121 35 Prague 2, Czech Republic  
pisa@cmp.felk.cvut.cz, <https://orcid.org/0000-0003-3476-5151>

**Abstract**—This paper deals with the explicit model predictive control (MPC) algorithms for permanent magnet synchronous motors (PMSM). The algorithms generate continuous and smooth set of pre-computed control laws represented by parameterized gains. The selection and application of the gains in real motion control of PMSM is explained. The MPC design introduces cost functions and control laws that define explicit algorithms. For this purpose, a unified state-space model of PMSM is proposed. In the paper, practical aspects of considered explicit MPC algorithms are investigated for control systems with floating-point arithmetic and usual incremental position sensors with quantized values. The proposed solution is demonstrated by real experiments with 95 W PMSM controlled by Field-Programmable Gate Array (FPGA) unit.

**Index Terms**—predictive control, FPGA, permanent magnet motors, control design, position control, velocity control

## I. INTRODUCTION

A lot of modern industrial, home and traffic applications are designed with effort to minimize mechanical elements transmitting power between drives and driven system, i.e. to use direct-drive concept. In this context, permanent magnet synchronous motors (PMSM) are frequently used. They have convenient construction (few mechanical elements) and adequate controllability (wide operation and loading ranges).

The control of PMSM is realized by two basic vector control strategies [1], namely Field-Oriented Control (FOC) in [2] and direct control (direct converter, finite-set control of speed, torque, current or power) in [3]–[6]. In spite of the faster response of the direct control, FOC, e.g. by model predictive control (MPC) [7], can more fit a PMSM motion especially in industrial applications with robotic systems, manipulators as it is e.g. in [8], where reference profiles are sophisticated time-parameterized curves [9]. The FOC principle consists in the design of appropriate amplitude and phase of stator voltage vector. The amplitude and phase are inputs to the Pulse-Width-Modulation (PWM) that provides appropriate voltage distribution in stator windings. The voltages excite adequate amplitude and frequency of Alternate Currents (AC) of the stator and generate motion and torque in the rotor. The FOC approaches include usual cascade PI control [2], [10] with dedicated MPC concept [11], and more general, MPC torque techniques [7], [12], multiparametric quadratic programming optimisation [13] or explicit MPC [14], [15], based on the primary concept of generalized predictive control (GPC) [16].

978-1-7281-9023-5/21/\$31.00 © 2021 IEEE

The paper follows up on our previous works [15], [17]. It introduces a novel unified model, specific fast procedure for online control law selection and practical notes for direct hardware implementation. At first, in Section II, the unified mathematical model is proposed for both position and speed control tasks so that a single control algorithm can also be used. The required task is selected by controller parameters only. In Section III, MPC concept with appropriate cost functions and optimisation criterions employing the unified model is described. Consequently, in Section IV, appropriate explicit control laws and off-line generation of gain profiles are explained. Simultaneously, a selection procedure for efficient picking from continuous stored off-line pre-computed gain profiles is introduced. The proposed procedure fits the gain profiles by parametric curves. It provides the fast gain selection by only single independent parameter in comparison with a discontinuous gain selection according to the state vector with minimally four variables [7]. Finally, Section V deals with the implementation issues of off-line design and storing of the gain profiles and on-line evaluation of the explicit control laws with the gains determined from the stored profiles. Real experiments are demonstrated in Section VI using 95 W PMSM drive controlled by novel FPGA unit involving the proposed predictive algorithms.

## II. UNIFIED MODEL FOR CONTROL DESIGN

PMSM model is given by the voltage distribution in appropriate AC phase system and by torque equilibrium equation, see [18], [19]. With Clarke and Park transformation, the model in  $d$ - $q$  rotating field coordinate system (reference frame) is:

$$u_{Sd} = R_S i_{Sd} + L_d \frac{d}{dt} i_{Sd} - L_q \omega_e i_{Sq} \quad (1)$$

$$u_{Sq} = R_S i_{Sq} + L_q \frac{d}{dt} i_{Sq} + L_d \omega_e i_{Sd} + \psi_M \omega_e \quad (2)$$

where  $R_S$ ,  $L_d$ ,  $L_q$  and  $\psi_M$  are stator resistance,  $d$ - $q$  inductances and rotor magnetic flux respectively (motor parameters);  $u_{Sd}$ ,  $u_{Sq}$  are  $d$ - $q$  voltages (system inputs);  $i_{Sd}$ ,  $i_{Sq}$  are  $d$ - $q$  currents;  $\omega_e$  is the electrical rotor speed (mechanical speed is  $\omega_m = \omega_e/p$ , where  $p$  is a number of pole pairs),

$$J \frac{d^2 \vartheta_e}{dt^2} = \frac{3}{2} p^2 (\psi_M i_{Sq} + (L_d - L_q) i_{Sd} i_{Sq}) - B \omega_e - p \tau_L \quad (3)$$

where  $J$  and  $B$  are moment of inertia and friction coefficient;  $\vartheta_e$  is the electrical rotor position; and  $\tau_L$  is a load torque.

The individual expressions (1), (2) and (3) can be rearranged into one unified state-space model as follows:

$$\begin{aligned} \frac{d}{dt} x(t) &= A_c(\omega_e) x(t) + B_c u(t) \\ y(t) &= C x(t) \end{aligned} \quad (4)$$

where  $x(t)$  and  $y(t)$  are state and output vectors defined below and  $A_c(\omega_e)$  and  $B_c$  are state and input matrices as follows

$$A_c(\omega_e) = \begin{bmatrix} -\frac{R_S}{L_d} & \frac{L_q}{L_d} \omega_e & 0 & 0 & 0 \\ -\frac{L_d}{L_q} \omega_e & -\frac{R_S}{L_q} & -\frac{\psi_M}{L_q} & 0 & 0 \\ 0 & \frac{3}{2} \frac{p^2}{J} \psi_M & -\frac{B}{J} & 0 & -\frac{p}{J} \\ 0 & 0 & 1 & 0 & 0 \\ 0 & 0 & 0 & 0 & 0 \end{bmatrix}, B_c = \begin{bmatrix} \frac{1}{L_d} & 0 \\ 0 & \frac{1}{L_q} \\ 0 & 0 \\ 0 & 0 \\ 0 & 0 \end{bmatrix} \quad (5)$$

Assuming the same inductances  $L_d \approx L_q$  and adequate compensation of passive, flux current  $i_{sd} \rightarrow 0$ , similarly for surface-mounted magnet structures, these matrices are

$$A_c(\omega_e) = \begin{bmatrix} -\frac{R_S}{L_S} & \omega_e & 0 & 0 & 0 \\ -\omega_e & -\frac{R_S}{L_S} & -\frac{\psi_M}{L_S} & 0 & 0 \\ 0 & \frac{3}{2} \frac{p^2}{J} \psi_M & -\frac{B}{J} & 0 & -\frac{p}{J} \\ 0 & 0 & 1 & 0 & 0 \\ 0 & 0 & 0 & 0 & 0 \end{bmatrix}, B_c = \begin{bmatrix} \frac{1}{L_S} & 0 \\ 0 & \frac{1}{L_S} \\ 0 & 0 \\ 0 & 0 \\ 0 & 0 \end{bmatrix} \quad (6)$$

considering single value of inductances  $L_S \equiv L_d = L_q$ . Remaining output matrix  $C$  determines required task: speed control  $C \equiv C_s$  or position control  $C \equiv C_p$  as follows

$$C_s = \begin{bmatrix} 1 & 0 & 0 & 0 & 0 \\ 0 & 1 & 0 & 0 & 0 \\ 0 & 0 & 1 & 0 & 0 \end{bmatrix}, C_p = \begin{bmatrix} 1 & 0 & 0 & 0 & 0 \\ 0 & 1 & 0 & 0 & 0 \\ 0 & 0 & 0 & 1 & 0 \end{bmatrix} \quad (7)$$

for speed control with output  $y = [i_{sd}, i_{sq}, \omega_e]^T$  and for position control with output  $y = [i_{sd}, i_{sq}, \vartheta_e]^T$ , respectively.

Thus  $A_c(\omega_e)$  is a varying state matrix with parameter  $\omega_e$ ;  $B_c$  is a constant input matrix; and  $C$  is a constant output matrix with unit elements in compliance with the required task and  $[i_{sd}, i_{sq}, \omega_e, \vartheta_e, \tau_L]^T$  is a state vector  $x(t)$ .

Note, that the two nonlinear terms  $\omega_e i_{sq}$  and  $\omega_e i_{sd}$  in (1) and (2) respectively are decomposed in (5) and (6) as in [19]. The rest nonlinear term  $i_{sd} i_{sq}$  in (3) is omitted in (5) with the assumption just below (5). The appropriate unified state-space model (4) is the initial model for the control design, i.e. it keeps one structure and identical dimensions for both speed and position tasks.

### III. PREDICTIVE CONTROL DESIGN

#### A. Definitions of MPC Design

This section outlines essential design terms. A used notation considers several principal variables:

$$\Delta x, x, \Delta y, y, \Delta u, u, e, w.$$

They represent increments and absolute values of the system state, system outputs, control actions  $u = [u_{sd}, u_{sq}]^T$ , errors and references  $w = [w_{isd}, w_{isq}, w_{\omega_e}]^T$  or  $w = [w_{isd}, w_{isq}, w_{\vartheta_e}]^T$  respectively. All variables are considered and defined as vectors respecting general multidimensional character of the PMSM model described in Section II.

The MPC algorithms are derived in discrete-time domain for direct digital implementation. Hence, the MPC design is evaluated for discretized state-space model (4) as follows:

$$\begin{aligned} \hat{x}_{k+1} &= A_d(\omega_{ek}) x_k + B_d(\omega_{ek}) u_k \\ y_k &= C x_k \end{aligned} \quad (8)$$

where  $A_d(\omega_{ek}) = e^{A_c(\omega_{ek})Ts}$

$$\text{and } B_d(\omega_{ek}) = (A_c(\omega_{ek}))^{-1} (e^{A_c(\omega_{ek})Ts} - I_{n_x}) B_c$$

subject to

$$\begin{aligned} y_{min} &\leq y_j \leq y_{max}, (C x_{min} \leq C x_j \leq C x_{max}) \\ u_{min} &\leq u_j \leq u_{max} \\ y_j &= w_j, (C x_j = w_j) \end{aligned} \quad (9)$$

at all time instants  $j > 0$  and  $k > 0$ , where the index  $j$  gradually falls within finite intervals of the time instants  $j = k, \dots, k + N$ , where  $k$  represents an initial time instant of the appropriate topical finite interval determined by prediction horizon  $N$  and  $\hat{x}_*$  is a prediction of state  $x_*$ .

In (8),  $A_d(\omega_{ek})$  is a varying state matrix with respect to the speed  $\omega_e$ .  $B_d(\omega_{ek})$  is a varying input matrix as well. These matrices are determined by the discretization in [20], as indicated.  $I$  is identity matrix of order equal to number of states  $n_x$ .  $C$  is a constant output matrix. It is identical for both continuous and discrete-time domains. Hence, MPC design has to be evaluated for values of speed  $\omega_e$  from its operating range  $\Omega_e \subset \mathbb{R}$ . It determines matrices  $A_d(\omega_e)$  and  $B_d(\omega_e)$ .

To achieve incremental and integrative character of MPC that suppresses undesirable steady-state error, the model (8) can be written in an incremental form. For simplicity of further notation only, let us write  $A_d \equiv A_d(\omega_{ek})$  and  $B_d \equiv B_d(\omega_{ek})$  keeping dependence on  $\omega_e$  without any change. Then, incremental form of the model (8) is:

$$\begin{aligned} \hat{x}_{k+1} - x_k &= A_d(x_k - x_{k-1}) + B_d(u_k - u_{k-1}) \\ \hat{y}_{k+1} - y_k &= C A_d(x_k - x_{k-1}) + C B_d(u_k - u_{k-1}) \end{aligned} \quad (10)$$

Hence, the final condensed form of the incremental model can be written as follows using difference  $\Delta^* j = j - j_{-1}$

$$\begin{aligned} \Delta \hat{x}_{k+1} &= A_d \Delta x_k + B_d \Delta u_k \\ \Delta \hat{y}_{k+1} &= C A_d \Delta x_k + C B_d \Delta u_k \end{aligned} \quad (11)$$

This modification will be used in MPC design to obtain one discrete integrator. In addition to the discrete model (8) or (11), an evolution model of aggregated control error  $\bar{e}_k$  is considered

$$e_k = w_k - y_k, \quad \bar{e}_k = \bar{e}_{k-1} + e_k \quad (12)$$

This modification will be used as a second discrete integrator.

To suppress steady-state error, one integrator is suitable for zero-order (step) reference signals and two integrators are suitable for first-order (ramp) reference signals. Moreover, two integrators correspond to usual cascade PI control in [1]. From practical point of view, the former modification is sufficient for static or slow-varying applications working with a finite set of reference points, the latter modification is sufficient for majority of dynamic applications as continuous motion control along continuous reference trajectories.

Furthermore, let us define time sequences (sequence vectors of variables)  $\Delta\hat{Y}_{k+1}$ ,  $\hat{Y}_{k+1}$ ,  $\Delta U_k$ ,  $W_{k+1}$ ,  $\hat{E}_k$  and  $W_{sk}$ , arising in the MPC design, as follows:

$$\Delta\hat{Y}_{k+1} = [\Delta\hat{y}_{k+1}^T, \Delta\hat{y}_{k+2}^T, \dots, \Delta\hat{y}_{k+N}^T]^T \quad (13)$$

$$\hat{Y}_{k+1} = [\hat{y}_{k+1}^T, \hat{y}_{k+2}^T, \dots, \hat{y}_{k+N}^T]^T \quad (14)$$

$$\Delta U_k = [\Delta u_k^T, \Delta u_{k+1}^T, \dots, \Delta u_{k+N-1}^T]^T \quad (15)$$

$$W_{k+1} = [w_{k+1}^T, w_{k+2}^T, \dots, w_{k+N}^T]^T \quad (16)$$

$$\hat{E}_k = [\bar{e}_k^T, \hat{e}_{k+1}^T, \dots, \hat{e}_{k+N-1}^T]^T \quad (17)$$

$$W_{sk} = [0^T, w_{k+1}^T, (\sum_{i=1}^2 \{w_{k+i}\})^T, \dots, (\sum_{i=1}^{N-1} \{w_{k+i}\})^T]^T \quad (18)$$

Finally, control parameters  $Q_{YW}$ ,  $Q_{\Delta Y}$  and  $Q_{\Delta U}$  are:

$$Q_{\diamond} = \begin{bmatrix} Q_*^T Q_* & & 0 \\ & \ddots & \\ 0 & & Q_*^T Q_* \end{bmatrix} \begin{array}{l} \text{subscripts } \diamond, * : \\ \diamond \in \{YW, \Delta Y, \Delta U\} \\ * \in \{yw, \Delta y, \Delta u\} \end{array} \quad (19)$$

which weigh individual terms in a MPC criterion.

### B. Optimality Criterion and Quadratic Cost Functions

In this paper, the design criterion is defined as follows

$$\min_{\Delta U_k} J_k(\hat{Y}_{k+1}, \Delta\hat{Y}_{k+1}, \Delta U_k, W_{k+1}) \quad (20)$$

$$\text{subject to: } \Delta\hat{x}_{k+j} = A_d \Delta\hat{x}_{k+j-1} + B_d \Delta u_{k+j-1},$$

$$\Delta\hat{y}_{k+j} = C \Delta\hat{x}_{k+j}, \quad \forall j = 1, \dots, N$$

$$(y_{min} =) C x_{min} \leq C x_j \leq C x_{max} (= y_{max}),$$

$$u_{min} \leq u_j \leq u_{max} \text{ and } \omega_{ek} = x(3)_k \text{ for } A_d \text{ and } B_d$$

where  $x(3)_k$  denotes the third element of the state vector  $x_k = [i_{sd}, i_{sq}, \omega_e, \vartheta_e, \tau_L]^T$  in the recent time instant  $k$ . Thus, one particular value  $\omega_e$  serves for the determination of matrices  $A_d$  and  $B_d$  for a computation of corresponding control-law gains within one particular prediction horizon  $N$ . Appropriate cost function in (20) is expressed for one involved integrator leading to the first MPC algorithm

$$J_k = (\hat{Y}_{k+1} - W_{k+1})^T Q_{YW} (\hat{Y}_{k+1} - W_{k+1}) + \Delta\hat{Y}_{k+1}^T Q_{\Delta Y} \Delta\hat{Y}_{k+1} + \Delta U_k^T Q_{\Delta U} \Delta U_k \quad (21)$$

or for two integrators leading to the second MPC algorithm

$$J_k = (\hat{Y}_{k+1} - W_{k+1} - \hat{E}_k)^T Q_{YW} (\hat{Y}_{k+1} - W_{k+1} - \hat{E}_k) + \Delta\hat{Y}_{k+1}^T Q_{\Delta Y} \Delta\hat{Y}_{k+1} + \Delta U_k^T Q_{\Delta U} \Delta U_k \quad (22)$$

A number of discrete integrators will be obvious from MPC algorithms summarized in the following subsection.

### C. Explicit MPC Algorithms

Using definitions in [15] and cost functions (21) and (22), the off-line minimisation of (20)  $\frac{dJ_k}{d\Delta u_k} = 0$  leads to the explicit MPC control laws used on-line:

- first MPC algorithm (one discrete integrator)

$$\Delta u_k := K_e(\omega_{ek}) (W_{k+1} - [I, \dots, I]^T y_k) - K_{\Delta x}(\omega_{ek}) \Delta x_k \quad (23)$$

$$u_k := u_{k-1} + \Delta u_k \quad (24)$$

- second MPC algorithm (two discrete integrators)

$$\bar{e}_k := \bar{e}_{k-1} + w_k - y_k \quad (25)$$

$$\Delta u_k := K_{\bar{e}}(\omega_{ek}) \bar{e}_k + K_{WL}(\omega_{ek}) W_{k+1} - K_y(\omega_{ek}) y_k - K_{\Delta x}(\omega_{ek}) \Delta x_k \quad (26)$$

$$u_k := u_{k-1} + \Delta u_k \quad (27)$$

where  $K_e(\cdot)$ ,  $K_{\Delta x}(\cdot)$ ,  $K_{\bar{e}}(\cdot)$ ,  $K_{WL}(\cdot)$  and  $K_y(\cdot)$  are gains for current value  $\omega_{ek}$ . New gain label  $K_{WL}(\omega_{ek})$  arises from the following rearrangement

$$K_{WL}(\omega_{ek}) W_{k+1} = K_W(\omega_{ek}) (I + L) W_{k+1} = K_W(\omega_{ek}) (W_{k+1} + W_{sk}) \quad (28)$$

where matrix  $L = [tril(1_N, -1) \otimes I_{n_y}]$  includes sums indicated in  $W_{sk}$ ,  $tril$  is a lower triangular selection from matrix of ones of order  $N$  on the  $-1$  diagonal and below, and  $\otimes$  denotes Kronecker product with identity matrix  $I$  of  $n_y$  order equivalent to motor outputs, see Sec. II, above (7). The gain values have continuous and smooth profiles, domains of which are identical with range  $\Omega_e$  ( $\omega_{ek} \in \Omega_e$ ) relating to a specific PMSM application. Note that the constrains (9) in (20) are solved independently according to [15], [21].

## IV. GAIN-SELECTION FROM EXPLICIT SETS

Let us consider for simplicity the first MPC algorithm with only two gains  $K_e(\omega_e)$  and  $K_{\Delta x}(\omega_e)$ . The gain  $K_e(\omega_e)$  depends on the length of prediction horizon  $N$ , i.e.  $K_e(\omega_e)$  is a matrix of type  $\mathbb{R}^{(2,3N)}$ , whereas  $K_{\Delta x}(\omega_e)$  is a matrix of fixed type  $\mathbb{R}^{(2,5)}$ . An example of the gain profiles and approximations is shown in Fig. 1 and Fig. 2.

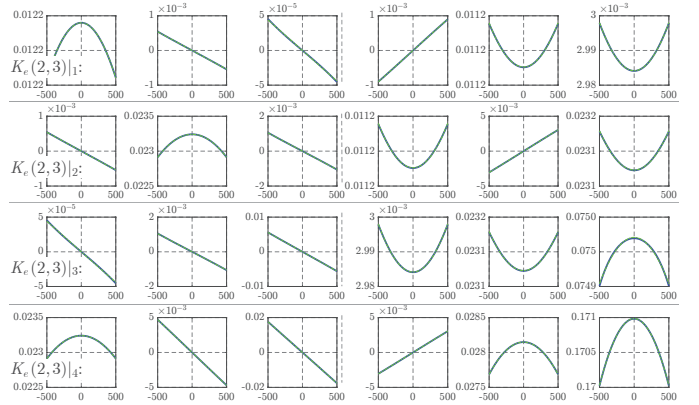


Fig. 1. Gain profiles  $K_e(\omega_e)(2,3N) = [k_e(i=1,2; j=(1,2,3) + 3(k-1))|_{k=1,\dots,N}]$ ;  $N=4$  (in rows).

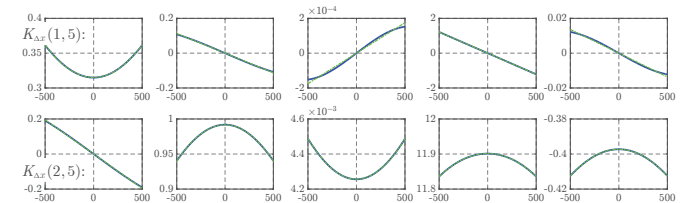


Fig. 2. Gain profiles  $K_{\Delta x}(\omega_e)(2,5) = [k_{\Delta x}(i=1,2; j=1,2,\dots,5)]$ .

The profiles of individual gain elements are continuous and smooth. They can be simply selected using polynomials with only one parameter  $\omega_e$ . The orders of the polynomials depend on curve shapes. However, for PMSM drives, the second-order polynomials are sufficient:

$$k_{(\cdot),i,j} = p(\omega_e) = p_{(0,i,j)} + p_{(1,i,j)} \omega_e + p_{(2,i,j)} \omega_e^2 \quad (29)$$

$$= p_{(0,i,j)} + \omega_e (p_{(1,i,j)} + p_{(2,i,j)} \omega_e)$$

where indexes  $i, j$  correspond to the types of gain matrices. Such selection gives appropriate explicit MPC gains from their pre-computed sets generally for whole operating range  $\Omega_e$  of the motor. Furthermore, it has reasonable memory demands since values for the whole  $\Omega_e$  are stored by finite number of coefficients of the polynomials  $p(\omega_e)$ , e.g. a number of the coefficients for the first algorithm is

$$(2 \times 3N) \times 3 \text{coeff.} + (2 \times 5) \times 3 \text{coeff.} \quad (30)$$

$$= (18N + 30) \text{coeff.}$$

i.e. for  $N = 4$ , the total number is 102 coefficients for 34 polynomials (29). The coefficients of the polynomials can be simply determined by MATLAB function 'polyfit':

$$p_{(0,1,2),i,j} = \text{polyfit}(\Omega_e, k_{(\cdot),i,j}, n) \quad (31)$$

The second order polynomial (29), i.e.  $n = 2$ , can describe arbitrary constant values, straight lines or parabola curves.

## V. IMPLEMENTATION

In this section, the real implementation will be described. This includes the following: the description of basic configuration or logical parts of the control unit with embedded explicit MPC algorithms defined in Section III-C, sensor quantization in off-line MPC design, description of used control unit LX\_RoCoN ([17]) and information on parameters of used PMSM. Discussed issues are generally applicable to PMSM and or BrushLess DC or AC motors, i.e. BLDC or BLAC motors.

### A. Block Diagram of MPC Implementation

The block diagram of the MPC implementation is shown in Fig. 3. The diagram corresponds to the real implementation in FPGA unit that will be described in Section V-B. The individual logical blocks of the diagram are as follows:

'Reference Signal Generator' generates reference values either for speed or position according to the required control task. Reference generation is given by simple time-parameterized polynomial profiles evaluated on-line, whereas reference composition is in fact lookup table value selection e.g. as in [9]. 'Position/Speed' block selects proper signals and ensures field weakening in speed control, [15].

'Predictive Control Law' block realises MPC control algorithms (23)-(24) and (25)-(27) including on-line gain selection by adequate polynomials (29) by the recent  $\omega_e$ .

Transformation blocks are represented by the expressions:

- 'Forward Clarke Transformation': currents

$$\begin{bmatrix} i_{S\alpha} \\ i_{S\beta} \end{bmatrix} = \begin{bmatrix} 1 & 0 & 0 \\ 0 & \frac{1}{\sqrt{3}} & -\frac{1}{\sqrt{3}} \end{bmatrix} \begin{bmatrix} i_{SA} \\ i_{SB} \\ i_{SC} \end{bmatrix} \quad (32)$$

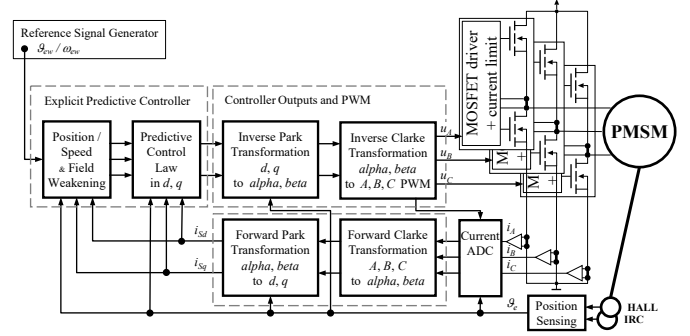


Fig. 3. Block diagram of MPC implementation.

- 'Forward Park Transformation': currents

$$\begin{bmatrix} i_{Sd} \\ i_{Sq} \end{bmatrix} = \begin{bmatrix} \cos \vartheta_e & \sin \vartheta_e \\ -\sin \vartheta_e & \cos \vartheta_e \end{bmatrix} \begin{bmatrix} i_{S\alpha} \\ i_{S\beta} \end{bmatrix} \quad (33)$$

- 'Inverse Park Transformation': voltages

$$\begin{bmatrix} u_{S\alpha} \\ u_{S\beta} \end{bmatrix} = \begin{bmatrix} \cos \vartheta_e & -\sin \vartheta_e \\ \sin \vartheta_e & \cos \vartheta_e \end{bmatrix} \begin{bmatrix} u_{Sd} \\ u_{Sq} \end{bmatrix} \quad (34)$$

- 'Inverse Clarke Transformation': voltages

$$\begin{bmatrix} u_{SA} \\ u_{SB} \\ u_{SC} \end{bmatrix} = \begin{bmatrix} 1 & 0 \\ -\frac{1}{2} & \frac{\sqrt{3}}{2} \\ -\frac{1}{2} & -\frac{\sqrt{3}}{2} \end{bmatrix} \begin{bmatrix} u_{S\alpha} \\ u_{S\beta} \end{bmatrix} \quad (35)$$

Prior to power blocks connecting control unit with real PMSM, it is desirable to suppress passive components of phase voltages. Such suppression can be done as follows

$$u_{\min} = \min(u_{SA}, u_{SB}, u_{SC})$$

$$u_{SA} = u_{SA} - u_{\min}$$

$$u_{SB} = u_{SB} - u_{\min}$$

$$u_{SC} = u_{SC} - u_{\min} \quad (36)$$

Note that this suppression is independent of a stator winding configuration (star or delta), but it corresponds to the rotor position. It also applies to currents in (32).

'Current ADC' is current analog-to-digital converter.

'HALL' is a HALL-effect sensor serving for initial approximate rotor position determination, i.e. the determining one of six sectors of the rotor.

'IRC' is an incremental rotary encoder sensor synchronized by HALL sensor with correction given by calibration index. This index relates to the electrical revolution of the rotor. IRC generates pulses corresponding to the recent increment of the rotor position  $\vartheta_e$  only.

'Position Sensing' block processes data of IRC and HALL sensors. The initial rough sector position of the rotor is given by HALL sensor. Once the index from IRC sensor appears, then the precise rotor alignment is maintained in this block. Since only position is available, relating speed  $\omega_e$  has to be estimated. For off-line control design as well as for on-line Explicit Predictive Controller laws, the sufficient estimation can be performed by backward Euler substitution

$$\omega_{ek} = \frac{\vartheta_{ek} - \vartheta_{ek-1}}{T_s} \quad (37)$$

Furthermore, during off-line control gain design stage, sensor quantisation should be emulated, i.e. simulated position should be quantised as follows

$$\bar{\vartheta}_{ek} = \frac{2\pi}{m_n} \text{round}\left(\frac{\vartheta_{ek} m_n}{2\pi}\right) \quad (38)$$

where  $m_n$  is a sensor resolution, i.e. number of marks per revolution. It leads to more conservative gain design more suitable for real use.

Finally, in on-line stage, the designed control actions according to (24) or (27) as well as instant increments of control errors  $\Delta\bar{e}_k = w_k - y_k$  in (25) have to be saturated with respect to the physically admissible PMSM behavior.

### B. Description of Used Control Unit

Control unit, used for MPC algorithm implementation, was LX\_RoCoN shown in Fig. 4, [17]. It consists of two boards, where one board serves for computation and outer communication and the second board is power board generating power signals for connected real PMSM:

- LX\_CPU board (size: 120×80×20 mm) NXP LPC4088 (Cortex-M3/M4F) with CPU Xilinx XC6SLX9 FPGA includes four IRC sensors interfaces with two phases, index and mark differential inputs per axis;
- LX\_PWR board (size: 130×100×40 mm) is isolated power stage with 16 power outputs/half-bridges up to 30 VDC and 5 A maximum current, DC/DC converter and helper supply for bridges with current measuring for each controlled output/phase.

### C. PMSM and its parameters used for experiments

For the real experiments in this paper, three-phase AC PMSM BLWR233D drive of the Anaheim Automation Co. is considered. Its catalogue parameters are listed in Table I. The parameters were verified by comparative simulation and experiment for free response on step signals of input voltages  $u_{Sd}$  and  $u_{Sq}$ .

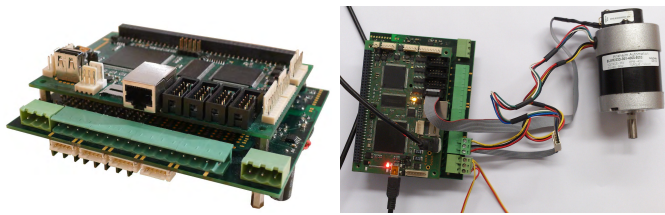


Fig. 4. Control Unit LX\_RoCoN ([17]) and PMSM.

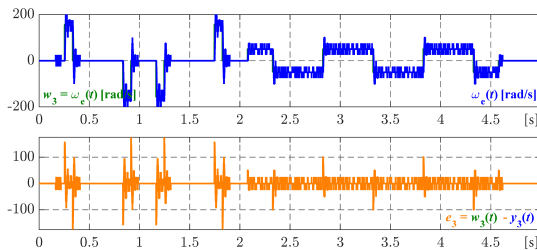


Fig. 5. Speed  $\omega_e$  and error  $e_3$  (first algorithm).

## VI. REAL EXPERIMENTS

As mentioned, real experiments were done on the PMSM BLWR233D with the control unit LX\_RoCoN, see Fig. 4. Initially, the experiment of speed control by the first MPC algorithm is in Fig. 5. It shows zero or zero-symmetric control error  $e_3$  in speed  $\omega_e$ . The used reference signal consists of zero-order steps only, therefore the first MPC algorithm with one discrete integrator is sufficient. Noticeable oscillation is caused by the sensor quantisation and speed estimation (37), but it does not influence the course of the position  $\vartheta_e$ . Further experiments are focused on the position control. The used reference signal consists of zero-order step and first-order ramp segments.

The results for the first MPC algorithm are demonstrated in Fig. 6. The left part of this figure shows the zero position error for the step segments of reference signals, but non-zero steady-state error for the ramp segments. The measured time histories of currents  $i_{Sd}$  and  $i_{Sq}$  (Fig. 6 in the middle) as well as the designed input voltages  $u_{Sd}$  and  $u_{Sq}$  (Fig. 6 on the right) are adequate with respect to step references and moderate in amplitudes. However, for the ramp signals, they are weak. Only one involved integrator is insufficient. Nevertheless, the first MPC algorithm is suitable as the energy efficient motion control for simple repeated manipulation operations that do not require accurate trajectory tracking but several steady positions. The results for the second MPC algorithm are demonstrated in Fig. 7. The left part of this figure shows that the position error tends to zero for the whole time interval of the position control experiment both for step and ramp segments of the reference signal. The position  $\vartheta_e$  closely follows these segments.

In case of sudden changes in the reference signal (sharp steps or sharp turns), slight overshoots occur. It is caused by the forceful effect of two discrete integrators in the control circuit. Time histories of input voltages  $u_{Sd}$  and  $u_{Sq}$  (designed control actions according to control laws (25) - (27), Fig. 6 and 7 on the right) correspond to this feature of the double integration. The input voltages are characterized by the sharp signal edges that can be slightly modified by the parameter  $Q_{\Delta u}$  in the appropriate cost function. The parameter  $Q_{\Delta u}$  determines the weight of the control action increment  $\Delta u$  compared with expected control error and other terms of the cost function.

From practical point of view, the managing of the motion control along the first-order ramp segments is sufficient for the majority of motion control applications, where coupled complex reference trajectories or individual reference signals of arbitrary order can or are usually approximated by first-order infinitesimal line segments.

## VII. CONCLUSION

The paper introduced the unified state-space model representation for speed and position motion control of PMSM drives by the explicit MPC algorithms. The detail description of low-cost implementation was addressed. Real experiments proved the proposed off-line computations and approximations

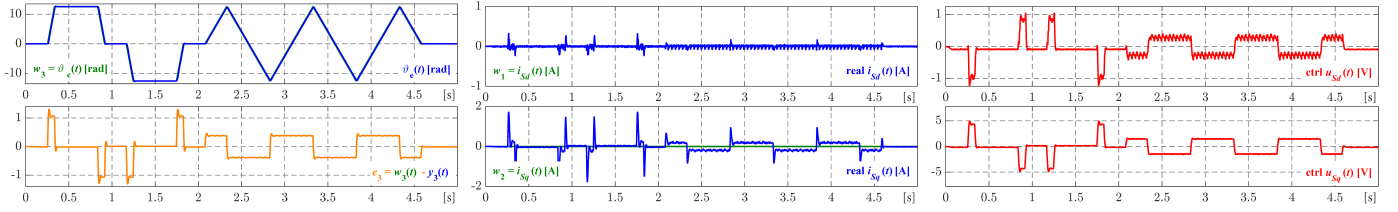


Fig. 6. Position  $\vartheta_e$  and error  $e_3$  (left); currents  $i_{sd}$  and  $i_{sq}$  (middle); and voltages  $u_{sd}$  and  $u_{sq}$  (right) (first algorithm).

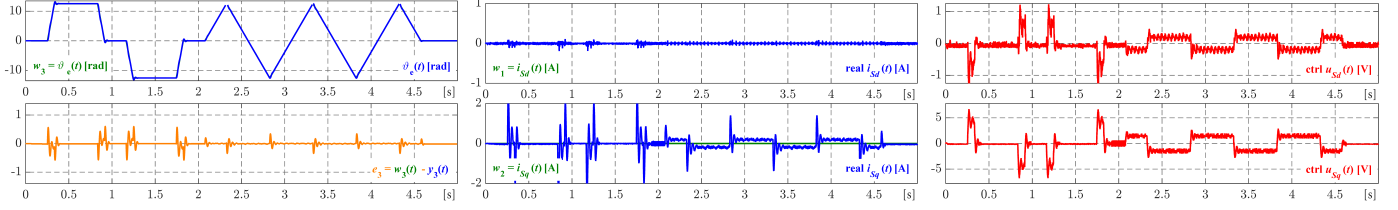


Fig. 7. Position  $\vartheta_e$  and error  $e_3$  (left); currents  $i_{sd}$  and  $i_{sq}$  (middle); and voltages  $u_{sd}$  and  $u_{sq}$  (right) (second algorithm).

TABLE I  
PARAMETERS: PMSM BLWR233D-36V-4000

Symbol	Description	Value
$P$	rated power	95 W (Watt)
$R_S$	stator resistance	0.64 $\Omega$ (Ohm)
$L_S$	stator inductance	0.0021 H (Henry)
$\Psi_M$	PM rotor magnetic flux	0.0200077 Wb (Weber)
$B$	viscous friction coef.	$\approx 0 \text{ kg}\cdot\text{m}^2\cdot\text{s}^{-1}$
$p$	number of pole pairs	4
$J$	moment of inertia	$1.1934\cdot 10^{-5} \text{ kg}\cdot\text{m}^2$

TABLE II  
PARAMETERS: FIRST MPC ALGORITHM

Symbol	Description	Speed Ctrl	Position Ctrl
$N$	horizon of prediction		4
$Q_{yw}$	out. penalization	diag(8, 4, 8)	diag(1, 1, 50)
$Q_{\Delta y}$	out. incr. penalization	diag(80, 600, 10)	diag(1, 5, 400)
$Q_{\Delta u}$	in. incr. penalization	diag(100, 250)	diag(3, 3)
$T_s$	sampling period		0.000250 s

TABLE III  
PARAMETERS: SECOND MPC ALGORITHM

Symbol	Description	Speed Ctrl	Position Ctrl
$N$	horizon of prediction		4
$Q_{yw}$	out. penalization	diag(16, 1, 6)	diag(1, 1, 60)
$Q_{\Delta y}$	out. incr. penalization	diag(1, 6, 40)	diag(1, 4, 600)
$Q_{\Delta u}$	in. incr. penalization	diag(200, 800)	diag(3, 3)
$T_s$	sampling period		0.000250 s

of the gains and on-line control by the explicit MPC laws based on the fast selection of the approximated gains.

## REFERENCES

- [1] P. Vas, *Sensorless vector and direct torque control*. Oxford Univ., 1998.
- [2] L. Wang, S. Chai, D. Yoo, L. Gan, and K. Ng, *PID and Predictive Control of Electrical Drives and Power Converters Using MATLAB / Simulink*, ser. IEEE Power Engineering Series. Wiley, 2015.
- [3] M. Preindl and S. Bolognani, "Model predictive direct speed control with finite control set of PMSM drive systems," *IEEE Trans. Power Electron.*, vol. 28, no. 2, pp. 1007–1015, 2013.
- [4] C. Xia, J. Zhao, Y. Yan, and T. Shi, "A novel direct torque control of matrix converter-fed PMSM drives using duty cycle control for torque ripple reduction," *IEEE Trans. on Ind. Electron.*, vol. 61, no. 6, pp. 2700–2713, 2014.
- [5] W. Xie *et al.*, "Finite-control-set model predictive torque control with a deadbeat solution for pmsm drives," *IEEE Trans. Ind. Electron.*, vol. 62, no. 9, pp. 5402–5410, 2015.
- [6] M. Siami, D. A. Khaburi, A. Abbaszadeh, and J. Rodríguez, "Robustness improvement of predictive current control using prediction error correction for permanent-magnet synchronous machines," *IEEE Trans. Ind. Electron.*, vol. 63, no. 6, pp. 3458–3466, 2016.
- [7] S. Bolognani, S. Bolognani, L. Peretti, and M. Zigliotto, "Design and implementation of MPC for electrical motor drives," *IEEE Trans. on Ind. Electron.*, vol. 56, no. 6, pp. 1925–1936, 2009.
- [8] A. Othman, K. Belda, and P. Burget, "Physical modelling of energy consumption of industrial articulated robots," in *15th Int. Conf. Control, Autom. and Systems*, 2015, pp. 784–789.
- [9] K. Belda and P. Novotný, "Path simulator for machine tools and robots," in *Int. Conf. MMAR*, 2012, pp. 373–378.
- [10] Siemens, *SINAMICS S120/S150, List Manual (LH1), 04, 6SL3097-4AP00-0BP5*, List Manual, Siemens, 2018.
- [11] T. Türker, U. Buyukkeles, and A. F. Bakan, "A robust predictive current controller for PMSM drives," *IEEE Trans. Ind. Electron.*, vol. 63, no. 6, pp. 3906–3914, 2016.
- [12] G. Cimini, D. Bernardini, A. Bemporad, and S. Levijoki, "Online model predictive torque control for permanent mag. synchron. motors," in *IEEE Int. Conf. on Indus. Technology*, 2015, pp. 2308–2313.
- [13] A. Bemporad, M. Morari, V. Dua, and E. N. Pistikopoulos, "The explicit solution of model predictive control via multiparametric quadratic programming," in *Proc. of American Control Conf.*, 2000, pp. 872–876.
- [14] S. Mariethoz, A. Domahidi, and M. Morari, "Sensorless explicit model predictive control of permanent magnet synchronous motors," in *IEEE Int. Electric Machines and Drives Conf.*, 2009, pp. 1250–1257.
- [15] K. Belda and D. Vošmik, "Explicit generalized predictive control of speed and position of PMSM drives," *IEEE Trans. Ind. Electron.*, vol. 63, no. 6, pp. 3889–3896, 2016.
- [16] A. Ordys and D. Clarke, "A state - space description for GPC controllers," *Int. J. Systems SCI.*, vol. 24, no. 9, pp. 1727–1744, 1993.
- [17] P. Píša, *LX\_RoCoN*, www.pikron.com, PiKRON Co., 2020.
- [18] L. Prokop and P. Grasblum, "3-phase PM synchronous motor vector control using a 56F80x, 56F8100, or 56F8300 device," Application Note AN1931, Freescale Semiconductor, 2005.
- [19] K. Belda, "Study of predictive control for permanent magnet synchronous motor drives," in *Int. Conf. Methods Models in Autom. Robotics*, 2012, pp. 522–527.
- [20] G. F. Franklin, D. J. Powell, and M. L. Workman, *Digital Control of Dynamic Systems*. Prentice Hall, 1997.
- [21] K. Belda, "On-line solution of system constraints in generalized predictive control design," in *Proc. of Int. Conf. on Process Control*, 2015, pp. 25–30.